Basic and Clinical
NEUROSCIENCE
May & June 2023, Volume 14, Number 3

Research Paper

Investigating the Glucagon-like Peptide-1 and Its Receptor in Human Brain: Distribution of Expression, Functional Implications, Age-related Changes and Species Specific Characteristics

Tulika Gupta[1*], Mandeep Kaur[1], Devendra Shekhawat[1], Ritu Aggarwal[2], Neha Nanda[2], Daisy Sahni[1]

1. Department of Anatomy, Post Graduate Institute of Medical Education and Research, Chandigarh, India.
2. Department of Immunopathology, Post Graduate Institute of Medical Education and Research, Chandigarh, India.

Use your device to scan and read the article online

Citation Gupta, T., Kaur, M., Shekhawat, D., Aggarwal, R., Nanda, N., & Sahni, D. (2023). Investigating the Glucagon-like Peptide-1 and Its Receptor in Human Brain: Distribution of Expression, Functional Implications, Age-related Changes and Species Specific Characteristics. *Basic and Clinical Neuroscience, 14*(3), 341-354. http://dx.doi.org/10.32598/bcn.2021.2554.2

http://dx.doi.org/10.32598/bcn.2021.2554.2

Article info:
Received: 23 Oct 2020
First Revision: 26 Dec 2020
Accepted: 06 Jan 2021
Available Online: 01 May 2023

Keywords:
Glucagon-like peptide-1, Glucagon-like peptide-1 receptor, Alzheimer disease, Human brain

ABSTRACT

Introduction: Emerging evidence has shown that the glucagon-like peptide-1 *(GLP-1)* agonist can be used to treat Alzheimer disease; however, knowledge of its neural targets is limited. To understand the neural substrates of *GLP-1*, we have done whole brain mapping for *GLP-1* and its receptor (*GLP-1R*), in 30 human brains.

Methods: *GLP-1* expression was studied by immuno-histochemistry and confirmed by the western blot method. The *GLP-1R* gene expression was studied by reverse transcription polymerase chain reaction.

Results: *GLP-1* expression was observed in most of the cortical areas (maximum in frontal, prefrontal and parietal cortex), diencephalon, and brainstem, but not in the cerebellum. Protein expression studies validated these results. The highest expression of *GLP-1R* was found in the frontal cortex. The orbitofrontal cortex and cerebellum had negligible expression. Hippocampus demonstrated a significant presence of *GLP-1R* but patchy immunoreactivity to *GLP-1*. *GLP-1R* presence in most of the human cortical regions and absence in the cerebellum is the major deviation from the animal brain. Sites that might be of interest in Alzheimer have been identified. *GLP-1* demonstrated an age-related decline in most of the areas after the fifth decade. At 60 years, *GLP-1* was not found in any of the cortical areas except in the prefrontal cortex; however, it was present in the sub-cortical areas.

Conclusion: Age-related profiling of *GLP-1* in various brain areas has been analyzed, which can have an important bearing on understanding Alzheimer disease. This study provides a detailed description of *GLP-1* and an brain mapping for the first time and may lead to novel treatment options targeting the *GLP-1* receptors.

*** Corresponding Author:**
Tulika Gupta*, *Associate Professor.
Address: *Department of Anatomy, Post Graduate Institute of Medical Education and Research, Chandigarh, India.*
Tel: *+91 (981) 5610227*
E-mail: *tulikag11@gmail.com*

Highlights

- Glucagon like peptide-1 *(GLP-1)* agonist can be used for treating Alzheime'rs disease.
- *GLP-1* gene expression was seen in cortical areas, diencephalon and brainstem, but not in cerebellum.
- Hippocampus demonstrated significant presence of *GLP-1R* but patchy immunoreactivity to *GLP-1*.
- *GLP-1* demonstrated age related decline in most of the areas after fifth decade.
- A detailed description of *GLP-1* and amp; *GLP-1R* locations was given which may lead to novel treatment options.

Plain Language Summary

Emerging evidence has shown that the glucagon like peptide-1 (*GLP1-1*) agonist can be used for treating Alzheimer's disease but knowledge of its neural targets is limited. To understand the neural substrates of *GLP-1*, we have done whole brain mapping for *GLP-1* and its receptor (*GLP-1R*), in 30 human brains. *GLP-1* expression was studied by immuno-histochemistry and confirmed by western blot method. *GLP-1R* gene expression was studied by RT-PCR. *GLP-1* expression was seen in most of the cortical areas (maximum in frontal, prefrontal & amp; parietal cortex), diencephalon and brainstem, but not in cerebellum. Protein expression studies validated these results. Highest expression of *GLP-1R* was found in the frontal cortex. The orbito-frontal cortex and cerebellum had negligible expression. Hippocampus demonstrated significant presence of *GLP-1R* but patchy immunoreactivity to *GLP-1*. *GLP-1R* presence in most of the human cortical regions and absence in cerebellum is the major deviation from the animal brain. Sites which might be of interest in Alzheimer's have been identified. *GLP-1* demonstrated age related decline in most of the areas after 5 th decade. At 60 years *GLP-1* was not found in any of the cortical areas except in the prefrontal cortex but it was present in the sub-cortical areas. Age related profiling of *GLP-1* in various brain areas has been analysed, which can have important bearing on understanding the Alzheimer's. This study provides detailed description of *GLP-1* and ations by complete human brain mapping for the first time and may lead to novel treatment options targeting the *GLP-1* receptors.

1. Introduction

Glucagon-like peptide (*GLP-1*) is secreted by L cells of the intestine. It is classified as an incretin because it increases the glucose-dependent release of insulin in response to food. *GLP-1* increases the synthesis and secretion of insulin from the pancreatic β cells, inhibits the release of glucagon, has an anabolic effect on the liver, and exerts a cardio-protective effect. It can also produce satiety through its action on the nucleus of tractus solitarius and hypothalamus (Andersen & Knop, 2018; Drucker, 2018). *GLP-1* acts via a trans-membrane receptor (*GLP-1R*). *GLP-1R* agonists are currently being used as anti-diabetic drugs for several years (Gupta, 2013). Recent studies have shown that *GLP-1* agonists have neuro-protective properties (Gejl et al., 2016; Holubová et al., 2019; Nakajima et al., 2016; Salcedo et al., 2012). Many studies have proven the neuro-trophic effects of *GLP-1* or *GLP-1* receptor agonists on cellular and animal models of neurodegenerative diseases, such as Alzheimer disease, Parkinson disease, acute cerebrovascular disorders, and traumatic brain injury (Athauda & Foltynie, 2016; Batista et al., 2018; Gao et al., 2014). This strongly suggests that *GLP-1* and *GLP-1R* have a widespread distribution in anatomically and functionally distinct areas of the central nervous system. In a recent study by Farkas et al. in 2020, the localization of GLP-1R protein was determined in rat brain. Immunoreactivity was seen in the circumventricular organs and areas around the arcuate nucleus and nucleus tractus solitarii (Farkas et al., 2020). Moreover, neuronal profiles of *GLP-1R* were distinguished in the telencephalon, diencephalon, brainstem, and cerebellum. Graham et al. in 2020 reported *GLP-1R*-expressing cells in the lateral septum, hypothalamus, amygdala, bed nucleus of the stria terminalis, hippocampus, ventral midbrain, periaqueductal gray, and cerebral cortex of transgenic mice (Graham et al., 2020).

Detailed information about the *GLP-1* location and its potential sites of action is an important first step in evaluating the function of *GLP-1* in the brain. To the best of our knowledge, complete mapping of the human brain for *GLP-1* and its receptor has not been done. There have been few studies on *GLP-1* receptors (*GLP-1R*) in specific areas of the brain, which regulate feeding, namely the hypothalamus and brain stem. Complete mapping of brain *GLP-1* receptors was done first time in rodent brain by Gu et al. in 2013 which was followed by mapping of nonhuman primate brain by Heppner et al. in 2015 (Gu et al., 2013; Heppner et al., 2015). The majority of studies examining the central *GLP-1* effects have been performed on rodents (Trapp & Richards, 2013).

This study aims to provide detailed information about the location of *GLP-1* and its receptors in the human brain. In this study, the samples were taken from 14 different sites, encompassing the whole human brain. The gene expression pattern of *GLP-1R* was studied by quantitative polymerase chain reaction, while *GLP-1* was detected by immunohistochemistry (IHC) using specific monoclonal antibodies as well as by studying the protein expression pattern by Western blot. These sites can be pharmacologically manipulated for treating neurological disorders.

2. Materials and Methods

Study samples

This study was conducted on adult human brains (n=30), obtained from autopsy (within 4-6 h after death), after obtaining informed consent. The samples were collected from the following sites:

1. Cortex: Orbitofrontal cortex, medial frontal cortex, pre-frontal cortex, frontal cortex, parietal cortex, occipital cortex, temporal cortex, and hippocampus;

2. Diencephalon: Thalamus (area containing-medial dorsal nucleus and midline nucleus) and hypothalamus (area containing-paraventricular nucleus);

3. This study was a randomized controlled triauperior colliculus), pons (area containing-ventral tegmentum), medulla (area containing-Inferior olivary nucleus, raphe nuclei and pyramidal fibers)

4. Cerebellum.

The patients with a history of any neurological disease, diabetes, head injury, or brain surgery were excluded from the study. The brain samples were collected in saline solution. The samples were divided and preserved in 10% buffered formalin for IHC (n=30), RNA later for mRNA study at 4˚C (n=10), and frozen at -80˚C for protein expression study (n=10).

Tissue location confirmation

Each tissue was subjected to a detailed histological examination to confirm the exact location of the tissue being studied.

Study procedures

Messenger RNA (mRNA) expression of *GLP-1R* for different regions was studied by RT-PCR. Meanwhile, the protein expression was studied by Western blotting for validation. *GLP-1* localization was done by IHC.

RNA isolation and cDNA synthesis

Total RNA was isolated from the sample of fresh brain tissue stored in the RNA later with a commercially available kit (RiboPureÔ, Ambion, Life Technologies, USA), according to the manufacturer's instructions. The yield and purity of RNA were assessed via the spectrophotometer by measuring absorbance at 260 nm and 280 nm. The integrity of RNA was verified by denaturing agarose gel electrophoresis. RNA bands on the gel were visualized under UV light. The presence of 18S as well as 28S rRNA bands confirmed the good quality of the yield. A total RNA measuring 500 ng was used to generate the first strand cDNA as the initial step of a 2-step reverse transcriptase polymerase chain reaction. The contamination with genomic DNA was eliminated by pre-treatment of cellular RNA with DNase1 (Invitrogen, San Diego, CA). The synthesis of cDNA was performed using a commercially available kit according to the manufacturer's instructions. cDNA of each sample was amplified using primers of glyceraldehyde 3-phosphate dehydrogenase (*GAPDH*) to check the efficiency of reverse transcription.

Relative gene expression assay by reverse transcription polymerase chain reaction for expression of *GLP-1R*

The selection of the housekeeping gene, namely *GAPDH* and β-actin were properly validated with brain samples to determine that their gene expression is unaffected by the experimental treatment. Both were run against *GLP-1R*. The cycle threshold value and melt curve of *GAPDH* were the least variable among all the samples as compared to β-actin; therefore, it was selected as the housekeeping gene.

The quantitative polymerase chain reaction was performed using sequence-specific predesigned primers and housekeeping gene using SYBR green chemistry.

GLP-1R (XM_017010751.1):

Forward-5'ATCCAAACTGAAGGCCAATC3'

Reverse-5'AGCTGGACCTCATTGTTGA3'

GAPDH (NC_000012.12):

Forward-5'ACACCGCCCTGGATCTCATA3'

Reverse-5'ACGAACGTGTGCGGAATCTT 3'

Relative quantification of genes was carried out on LightCycler® 480 real-time polymerase chain reaction system (Roche Diagnostics, Germany). The amount of *GLP-1R* mRNA was normalized to *GAPDH*. The following cycling parameters were used: For 7 min at 95˚C followed by 40 cycles of 10 s at 95˚C and 30 s at 60˚C. The reaction volume was 10 µL. The analysis of data was done using the ΔCt method. To nullify the due variation in samples, the data were normalized to the housekeeping gene (*GAPDH*) which served as an internal control. The samples were loaded in triplicates. To calculate ΔCt, the average of triplicate cycle threshold values was taken and the mean cycle threshold value of *GAPDH* was subtracted from the mean cycle threshold value of the gene of interest (*GLP-1R*).

We have chosen to use ΔCt for analysis instead of ΔΔCt which is more commonly used. ΔΔCt can be calculated by comparing the change in the gene expression relative to the diseased case in the same organ (different areas of the brain in our case). We did not have diseased brain samples. Another method to calculate ΔΔCt is to use the expression of the same mRNA in another organ as a calibrator. It provides tissue comparison; however, the results are difficult to analyze from a biological point of view. The single relative quantity reported reflects variation in both target and reference transcripts across a variety of cell types that might be present in any particular tissue (Schmittgen & Livak, 2008). Given that this study aims to record the expression of the *GLP-1R* mRNA in different regions of the brain, which can be further used, we have chosen to present our results as ΔCt.

Western blot to check the protein expression of *GLP-1*

The tissue was incubated on ice for 15 min and lysed with chilled 1X RIPA lysis buffer and protease inhibitor (Merck-Millipore). The suspension was centrifuged at 14000 rpm for 25 min at 4˚C and the supernatant was collected. The protein concentration was determined by BCA assay using a bicinchoninic acid assay kit (Thermofisher Scientific). Meanwhile, 30 µg of the total protein sample was mixed with the 2X Laemmli's sample buffer and heated at 100˚C for 5 min. The protein samples were immediately put on the ice. Proteins were separated on 12% sodium dodecyl sulfate-polyacrylamide gel electrophoresis. For immune detection, total proteins on the gel were electro-transferred to a polyvinylidene difluoride membrane (Immobilon™-P, Millipore) using a trans-blot transfer cell (Bio-Rad). The polyacrylamide gel was stained with commassie brilliant blue (CBB) G-250 for 1 h and de-stained with double distilled water overnight. The membrane was blocked with 5% bovine serum albumin in the solution of tris-buffered saline and 0.1% Tween 20 (TBST) for 1 h at room temperature. The membrane was washed 3 times, 5 min each with TBST buffer and was incubated with primary antibody (anti-GLP-1, 1:1500 dilution, mouse monoclonal, ab36598) in 5% bovine serum albumin buffer overnight at 4˚C with β actin (anti-β actin, 1:5000 dilution, mouse monoclonal, MA5-15739) as control. The membrane was washed 3 times, 5 min each with TBST buffer followed by incubation with horseradish peroxidase-conjugated secondary antibody (anti-mouse, 1:40,000 dilution, ab97046). The membrane was again washed 3 times, 5 min each with TBST buffer. The visualization of the blot was done with enhanced chemiluminescence substrate (Bio-Rad laboratories, USA) by the protein simple imaging system.

The densitometric analysis was done using the Image J software by selecting the bandwidth and measurement of intensity. The quantification of the bands was then performed using β-actin as a control. The ratio of the area of interest/β-actin of the band intensities was taken.

Localization of *GLP-1* expression done by immunohistochemistry

For IHC, tissue sections were fixed in 10% buffered formalin, processed, and embedded in paraffin following a standard protocol. The sections were de-paraffinized and hydrated gradually through graded alcohols (100%, 70%, and 50%) and washed in de-ionized water. Endogenous blocking was done by hydrogen peroxide to quench endogenous peroxidase activity. Antigen was retrieved in citrate buffer at pH 6.1 for 12 min to increase immunogenicity. The slides were then incubated with *GLP-1* monoclonal (anti-GLP-1.5 µg/mL dilution, mouse monoclonal, ab36598) primary antibody at 4˚C overnight and followed by secondary antibody (anti-

mouse, 1:2000 dilution, Abcam, ab97046) for 1 h at room temperature. Peroxidase activity was developed in 0.5% 3, 3'-diaminobenzidine. Counterstaining was done with hematoxylin. Pancreatic tissue was used for positive control, and negative control was obtained by excluding the primary antibody. Sections were cleared in xylene and mounted with di-n-butyl phthalate in xylene.

3. Results

GLP-1 immunohistochemistry

As shown in Figure 1 and Figure 2, thirty tissue samples were divided into 3 groups, namely cases with, age less than 30 years in group 1 (group 1a: Up to 20 years and group 1b: >20 years), cases in the age range of 30 to 50 years in group 2 (group 2a: Up to 40 years and group 2b: >40 years), and cases more than 50 years in group 3 (group 3a: <60 years and group 3b: -60 years) (Table 1).

Group 1 (age<30 years)

Cortex: In 5 cases of the below 20 years age group (14-16 years), immunoreactivity to *GLP-1* monoclonal antibody was not observed in any region of the cerebral cortex. In cases from 20 to 30 years, immunoreactivity of mild intensity was detected in cortical regions in a patchy fashion. In the prefrontal cortex, patchy immunoreactivity was found in the large pyramidal cells and neuropil (data not shown). In frontal, parietal, and temporal cortical areas scattered immuno-staining of punctate cytoplasmic pattern was observed only in large pyramidal cells along with neuropil staining. The temporal cortex showed scanty immunoreactivity. No immunoreactivity was seen in the occipital cortex. Hippocampus staining was in a marginally extensive area, including few pyramidal cells in stratum pyramidal and scattered neuropil.

Diencephalon: The thalamic sample was taken from the magnocellular part of the medial dorsal nucleus and the midline nuclei. In group 1a, neurons were not stained but scattered mild immunoreactivity was seen in the white matter and choroid plexus. In group 1b, the IHC picture was the same but in a few places groups of 2-3 neurons were also stained. The hypothalamic sample was taken from the paraventricular nucleus (medial part), which showed scattered magnocellular neurons in the background of small neurons. Scanty mild immunoreactivity was seen in a few magnocellular neurons and all group 1 case.

Brain stem: In pons, small patches of mild immunoreactivity involving 1-2 pontine neurons were found. In the medulla, the tissue sample has been taken from the open part of the medulla as shown in Figure 2. This medullary tissue included the medial part of the inferior olivary nucleus, pyramidal fibers, and raphe nuclei of the medullary reticular formation. In the lateral part, corresponding to the central reticular nucleus of the medulla, mid-immunoreactivity patches encompassing 3-5 neurons and the surrounding neuropil were seen. The inferior olivary nucleus depicted mild immunoreactivity of neurons and hilar fibers. Pyramidal fibers were unstained.

Cerebellum: No immunoreactivity was seen in the cerebellum.

Group 2 (age 30-50 years)

Cortex: Immunoreactivity to *GLP-1* monoclonal antibody was observed in all areas of the cortex, though the quantity, intensity, and location pattern were variable. Scattered immunoreactivity involving cortical layers 2 to 6 was observed in all of the cortical areas The staining intensity was more in layers 3 and 5 where moderate staining was seen in the scattered areas involving 2-5 granule cells and their neuropil. Meanwhile, mild punctuate cytoplasmic staining was seen in some large pyramidal cells and their processes. The orbital frontal cortex was an exception to this because it only showed scattered mild immunoreactivity in the cortical layer 3. The cortical layer 1 was not stained in most of the areas except the medial frontal and parietal cortices. The least immunoreactivity was seen in the occipital cortex. The hippocampus showed moderate-intensity staining of patches of neuropil near the surface. The large pyramidal cells in stratum pyramidal showed moderate staining of cytoplasm and associated neurites at places.

Diencephalon: In the thalamus scattered immunoreactivity of mild to moderate intensity was seen, involving the fibers mainly but at places where neurons were also stained. Some large neurons showed cytoplasmic granular staining in part of the cytoplasm while in a few neurons, the immunoreactivity was seen in the whole of the cytoplasm and their arborization. The hypothalamic sample showed scattered magnocellular neurons in the background of small neurons. The small neurons did not take the stain. The magnocellular immunoreactivity was in the form of cytoplasmic stippling, forming a crescent, which variably covered 1/fourth, 1/third, or almost the whole cell.

Brain stem: In the medulla, the lateral part, corresponding to the central reticular nucleus of the medulla, had moderate immunoreactivity patches encompassing 3-5 neurons and the surrounding neuropil. This was the area

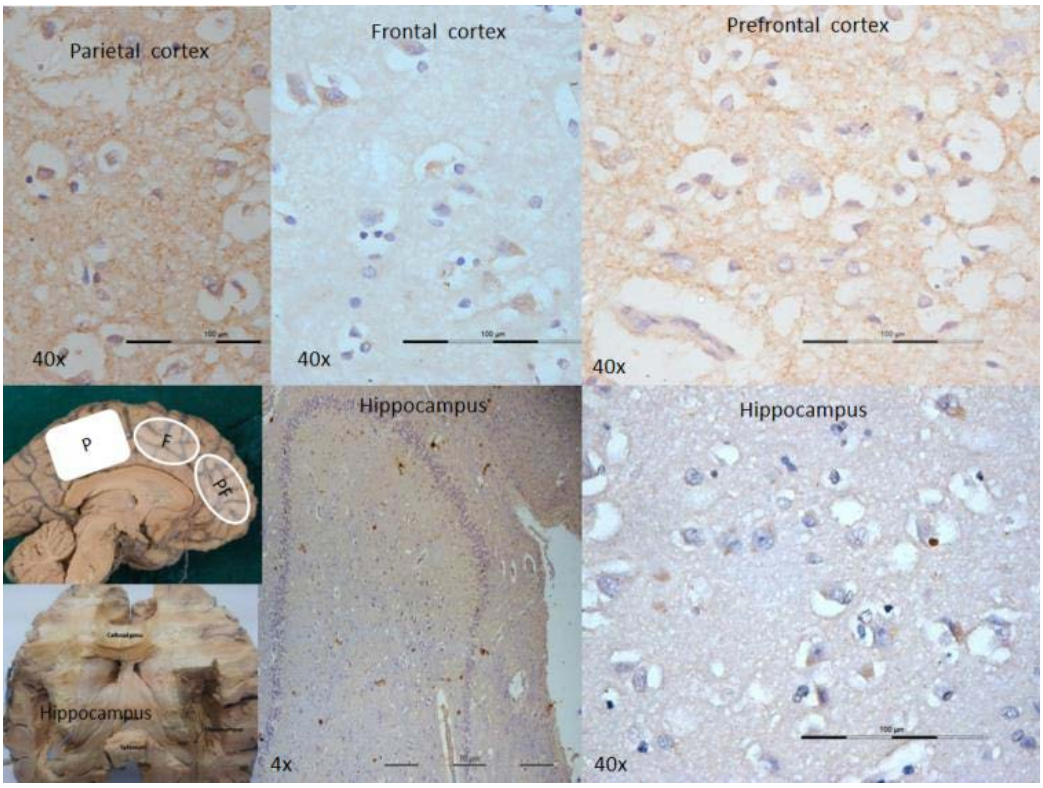

NEUROSCIENCE

Figure 1. Microscopic anatomy of various cerebral cortical areas after immunostaining using GLP-1 monoclonal antibody

Notes: The macroscopic view of the cerebrum in the mid-sagittal section depicts the prefrontal (PF), the frontal (F), and the parietal (P) cortical areas. Below that, an inferior view of the cerebrum, dissected to demonstrate the hippocampus is shown in the left lower corner. The parietal cortex at 40x magnification depicts moderate immune staining in the neuropil and scattered mild staining in neurons. The frontal cortex at 40x magnification depicts cytoplasmic staining in large pyramidal cells of cortical layer 5. The prefrontal cortex shows moderate immunoreactivity in the granule cells and surrounding neuropil, including a vessel wall. The hippocampal trilaminar cortex with scattered immunoreactivity is observed at 4x magnification. At 40x magnification, moderate patchy IR is seen in large pyramidal cells and few fibers in the stratum pyramidal of the Hippocampus.

of maximum immunoreactivity in the medullary tissue. An inferior olivary nucleus with a typical crumpled bag appearance was seen. Its neurons showed cytoplasmic punctate staining of moderate intensity, covering half of the total cellular area. Scattered patches of immunoreactivity, of moderate intensity, were also observed in the fibers seen at the hilum of the Inferior olivary nucleus. Pyramidal fibers were unstained. In the median part of the tissue, intense punctate staining was seen in the median raphe reticular nuclei. In pons, moderate intensity patchy staining of 4-8 pontine nuclei and nerve fibers around them was seen.

Cerebellum: No immunoreactivity was seen in the cerebellum

Group 3 (age>50 years)

The pattern of the IHC results in group 3a was similar to group 2, except for the variations in the intensity of immunoreactivity; the prefrontal, temporal, and hippocampal areas showed lesser intensity while higher intensity immunoreactivity was observed in the brain stem.

In group 3b, there was a major difference in cortical immunoreactivity because none of the cortical areas showed immunoreactivity, except the prefrontal cortex. The prefrontal cortex had mild staining, scattered in all the cortical layers, and in a few large pyramidal neurons and their processes. The diencephalon also depicted much lesser immunoreactivity in this group. Thalamus immunoreactivity was very mild and only fibers were stained. In the hypothalamus, mild immunoreactivity was seen in occasional magnocellular neurons covering half to ¾ of its cytoplasmic area. The immunoreactivity pattern was similar to group 2 but with decreased intensity.

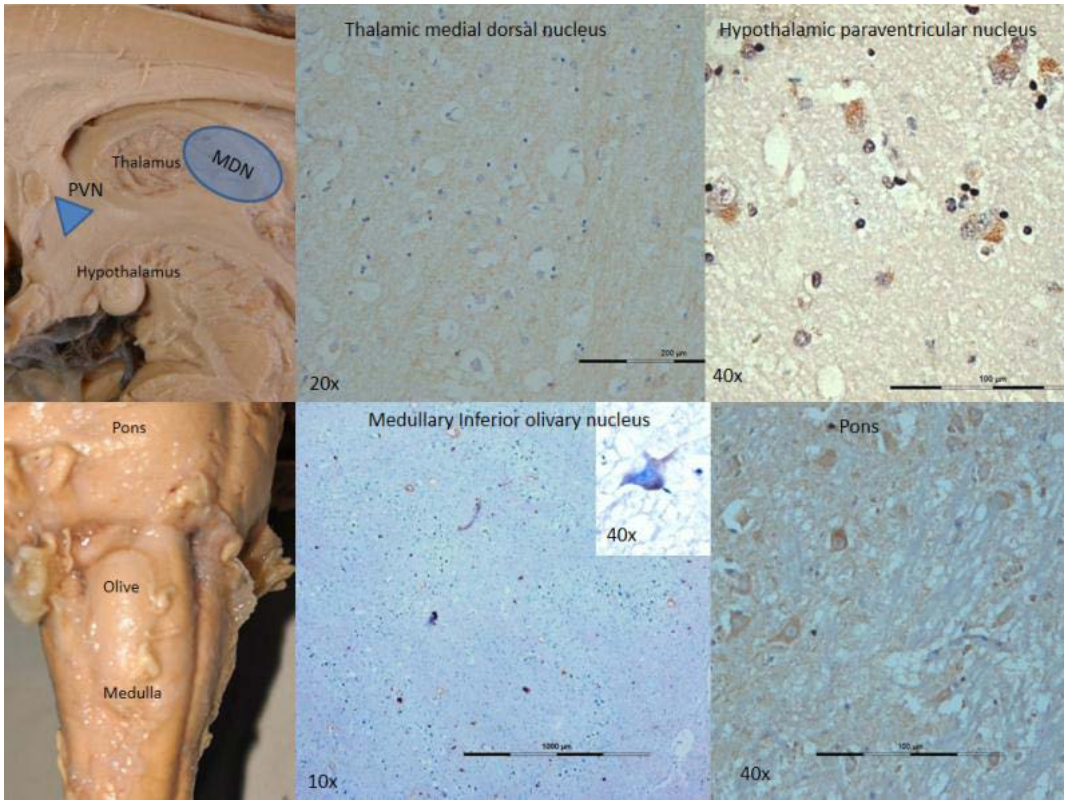

NEUROSCIENCE

Figure 2. The upper panel depicting macroscopic mid sagittal view of the thalamus and the hypothalamus

Notes: The diagrammatic representation of the thalamic medial dorsal nucleus (MDN) and the hypothalamic paraventricular nucleus (PVN) is shown in the section. The thalamic MDN at 20x magnification depicts moderated immunoreactivity in the fibers and a few large neurons. The hypothalamic PVN shows magnocellular neurons in the background of small neurons at 40x. immunoreactivity is seen in the magnocellular neurons as cytoplasmic stippling forming a crescent. Small neurons did not take the stain. The lower panel depicts a macroscopic view of the olive in the medulla, followed by the microscopic view of the inferior olivary nucleus. A typical crumpled bag appearance of the inferior olivary nucleus can be seen at 10x. In the inset, the pattern of staining in the neuron can be appreciated in the form of cytoplasmic punctate moderate intensity immunoreactivity, at 40x magnification. The pons at 40 x magnification shows a group of pontine nuclei and surrounding neuropil with moderate immunoreactivity. Immunostaining has been done using GLP-1 monoclonal antibody.

GLP-1 protein expression

As shown in Figure 3, to analyze the protein expression of *GLP-1*, separate regions from the human brain were classified into 4 groups. The quantification of Western blot images with the aid of the Image J software revealed that the ratios of the net band to net loading control (β-actin) for the regions of the first group i.e. orbitofrontal cortex, medial frontal cortex, and temporal cortex were 0.267, 0.76, and 0.619, respectively. The second group comprising proteins from the midbrain, medulla, and pons displayed ratios of 7.0, 3.77, and 6.22, respectively. For the third group (frontal cortex, prefrontal cortex, and parietal cortex) values of the ratios were obtained at 17.0, 11.2, and 5.2, respectively. The ratio of the intensities of the bands observed in the fourth group comprising of hippocampus, thalamus, and hypothalamus was calculated at 0.418, 0.905, and 0.108, respectively. When comparing all regions, the data revealed that the highest expression of *GLP-1* was found in the frontal cortex and the lowest in the hypothalamus. No results were found in the occipital cortex and cerebellum. This data is diagrammatically represented in Figure 3.

GLP-1 receptor

As shown in Figure 4, the gene expression of *GLP-1R* in 14 different brain regions was assessed in 10 cases (in the age range of 27 to 60 years). The brain regions included were the orbitofrontal cortex, medial-frontal cortex, pre-frontal cortex, frontal cortex, parietal cortex, occipital cortex, temporal cortex, hippocampus, thalamus, hypothalamus, midbrain, medulla, pons, and cerebellum. The mean delta cycle threshold values for these

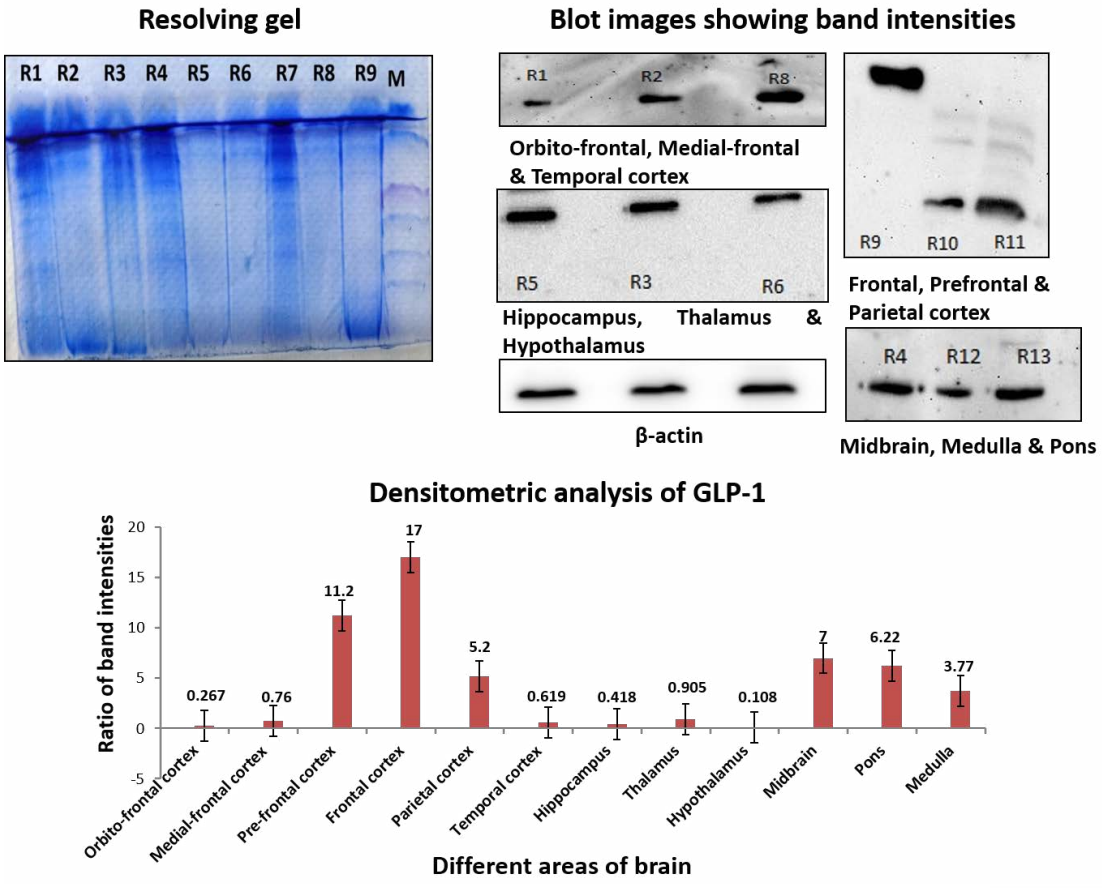

Figure 3. Total protein separated by SDS-PAGE, Resolved on 12% resolving gel, stained with Commassie blue

Notes: A total of 10 wells of gel was loaded with 9 samples and protein marker (M) of known molecular weight to check the presence of protein and their resolution. The representative images of the protein blot of different areas of the brain and β-actin, for *GLP-1* expression. At the bottom, a graphical representation of the GLP-1 protein expression is seen. Densitometric analysis was done using the Image J software by selecting bandwidth and measurement of intensity. The quantification of the bands was then performed using β-actin as a control. Each of the brain areas studied is shown on the X axis and the ratio of band intensities of the sample (from each brain area)/β-actin is shown on the Y axis.

regions were 0, 3, 12.92, 17, 13.35, 1.4, 1.58, 8.92, 7.8, 8.768, 12.25, 3.7, 8.408, and 0, respectively. The data revealed that the highest expression of *GLP-1R* was found in the frontal cortex. The pre-frontal cortex, midbrain, and parietal cortex have lower expression than the frontal cortex. Diencephalon, the hippocampus, and pons have moderate expression, whereas the medial frontal cortex, occipital cortex, temporal cortex, and medulla are expressed at low levels. Orbito-frontal cortex and cerebellum did not have any expression.

4. Discussion

In our study, the *GLP-1* expression was observed by dual methods and the results of the proteomics study are in line with the immuno-histochemical expressions. Moderate intensity IHC staining, observed in the pre-frontal cortex, frontal cortex, parietal cortex, and the brain stem is reflected in the quantified protein expression in these sites. Similarly in the hypothalamus, the amount of protein expressed is less, which is in line with the *GLP-1* immunoreactivity seen only in the scattered magnocellular neurons.

GLP-1R is a G protein-coupled receptor. mRNA coding for this receptor is widely expressed in rodents (Le et al., 2018; Merchenthaler et al., 1999; Ohshima et al., 2015; Reiner et al., 2016) and non-human primates (Heppner et al., 2015). We also found widespread gene expression of *GLP-1R* in the human brain. Most of the cerebral cortical regions and diencephalon expressed *GLP-1* mRNA, while the expression in the brainstem decreased inferiorly, with high expression in the midbrain, moderate in the pons, and low in the medulla.

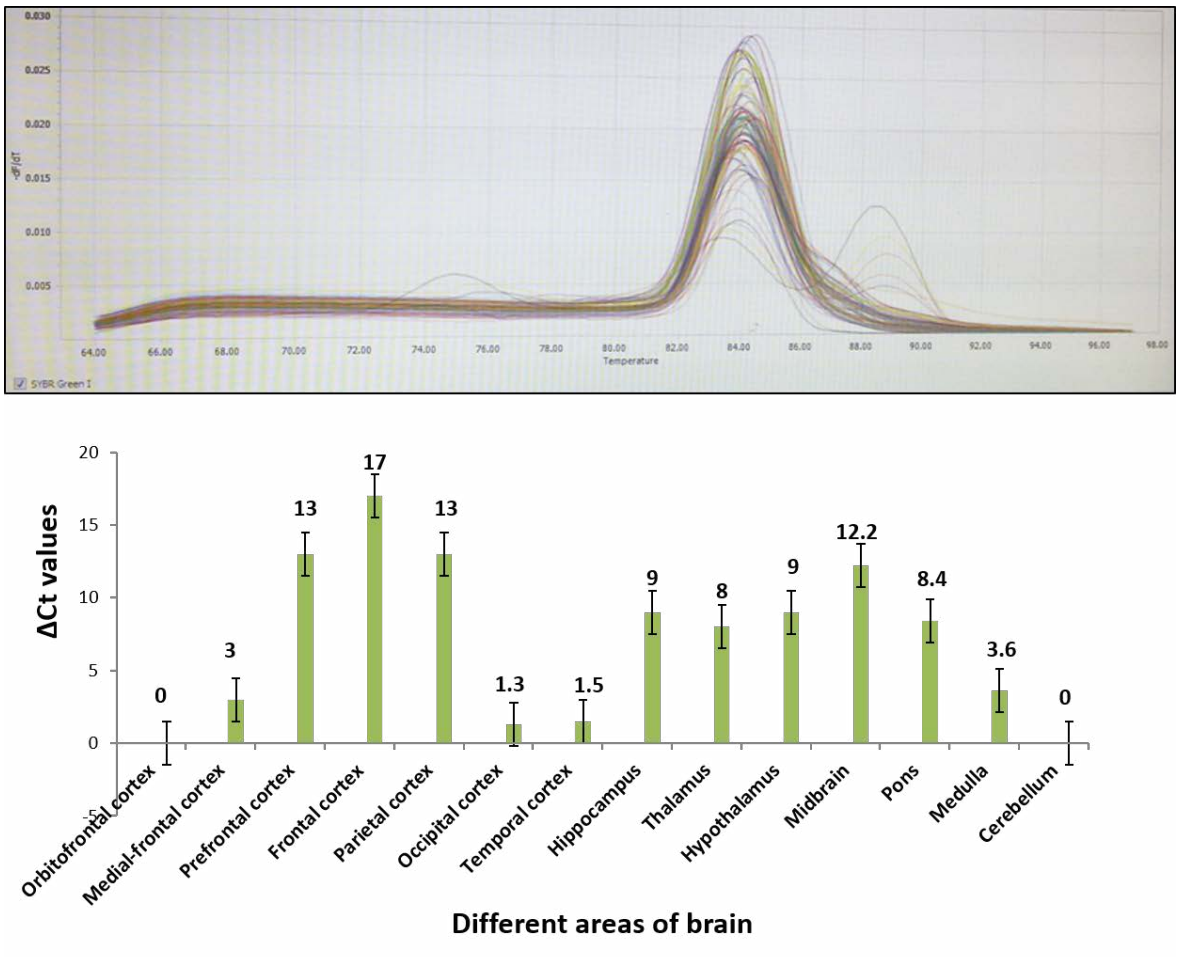

NEUROSCIENCE

Figure 4. In the upper panel, melt curve analysis is shown-performed at the end of the PCR cycle, to confirm the speci-ficityof primer annealing

In the lower panel, a graphical representation of the GLP-1 recep areas of the brain is shown. The Y axis represents the mean of delta cycle threshold values for these areas.

On comparing the gene expression profile of *GLP-1R* with the *GLP-1* sites mapped by immunoblotting and IHC, we observed that the *GLP-1* location profile matches its receptor location in most of the cortical areas and the brain stem. In the hippocampus and the diencephalon mRNA expression far exceeded the protein expression. This might indicate that the hippocampus and diencephalon are responsible for the production of *GLP-1* which is then transported to other sites. The IHC finding of moderate intensity staining of neuropil in the hippocampus supports this conclusion.

Functional considerations of *GLP-1* and *GLP-1R*

The distribution profile of *GLP-1* and its receptor found in the present study is consistent with possible areas of interest in Alzheimer disease. The pre-frontal and parietal cortices were found to have maximum *GLP-1* and *GLP-1R* concentrations. The prefrontal cortex is involved in planning, social insight, and judgment while the parietal cortex integrates, analyzes, and contextualizes sensory input. The hippocampus is responsible for new memory formation and retrieval of old memories in association with the prefrontal cortex (Preston & Eichenbaum, 2014). Both the thalamic nuclei which have shown moderate amounts of *GLP-1* and its receptor, in the present study, have behavioral functions. The thalamic medial dorsal nucleus lends an emotional tone to the behavior while midline nuclei are believed to play a role in memory. In the present study the hypothalamic paraventricular nuclei, which is considered to be a major area for energy homeostasis in the brain, showed moderate presence of *GLP-1* and *GLP-1R*. Reduced glucose utilization and disturbed energy metabolism occur early in the course of Alzheimer

Table 1. Demographic data of the studied cases

S. No	Age (y)/Gender		
	Group 1 <30	Group 2 30-50	Group 3 >50
1	14/F	30/M	51/M
2	15/M	31/M	52/F
3	15/M	32/M	52/M
4	16/M	38/M	53/M
5	16/M	40/M	60/M
6	20/M	40/F	60/M
7	22/M	42/M	60/M
8	24/F	45/M	60/M
9	27/M	45/M	60/M
10	29/M	47/M	
11		50/M	

M: Male; F: Female. NEUROSCIENCE

Table 2. Age-related decline in *GLP-1* immunoreactivity in human brain

Brain Area	Group 1 <30		Group 2 30-50		Group 3 >50	
	Up to 20	>20	Up to 40	>40	<60	60
Cerebral Cortex						
Prefrontal cortex	-	+	++	++	+	+
Frontal cortex	-	+	++	++	++	-
Parietal cortex	-	+	++	++	++	-
Temporal cortex	-	+	++	++	+	-
Hippocampal	-	+	++	++	+	-
Diencephalon						
Thalamus	+	+	+++	++	++	+
Hypothalamus	+	+	++	+++	+++	+
Brain Stem						
Midbrain	+	+	++	++	+++	++
Pons	+	+	++	+	+++	++
Medulla	+	+	++	++	+++	++

-No immunoreactivity, +Mild immunoreactivity, ++Moderate immunoreactivity, +++Intense immunoreactivity. NEUROSCIENCE

Table 3. Species-specific differences in *GLP-1* receptor

Brain Area	Human	Non-human Primate	Rodents
Cerebral cortex	Present in all areas, except the orbitofrontal cortex	Absent	Absent, except in mouse prefrontal cortex
Hippocampus	Present	Present	Present
Amygdala	Present	Present (much higher than rodents)	Present
Diencephalon			
Thalamus	Present	Present	Present
Hypothalamus	Present	Most abundant expression	Most abundant expression
Brain stem	Present	Present	Present
Cerebellum	Absent	Present	Present

NEUROSCIENCE

disease and correlate with impaired cognition (Monte, 2012; Simsir et al., 2018). Thus, the distribution pattern of *GLP-1* and its receptor described in this study provide an anatomical basis for the clinical observations made by many authors; accordingly, *GLP1-R* agonist might prove to be therapeutic in sporadic Alzheimer's disease (Gao et al., 2014; Gejl et al., 2016).

Age-related changes in *GLP-1*

As provided in Table 2, age-related decline in *GLP-1* in the human brain was also observed in the present study. *GLP-1* was absent in cortical areas, including the hippocampus below 20 years. From 20 to 50 years, it increased with age in all cortical areas studied; however, it started decreasing after the age of 50 years. At 60 years of age, immunoreactivity to the *GLP-1* was absent in all cortical areas, except in the prefrontal cortex. In the subcortical regions, positive immunoreactivity for *GLP-1* was observed as early as 13-18 years of age; subsequently, it increased with age until 55 years of age. At 55 years of age, about a 30% decline in the *GLP-1* immunoreactivity was noticed in all subcortical regions studied. These levels persisted until 60 years. At 60 years, *GLP-1* was seen in reduced amounts in the prefrontal cortex and subcortical areas only (we did not have any sample older than 60). Age-related reduction of *GLP-1* in mouse prefrontal cortex was demonstrated, which was found to be associated with impairment of spatial cognitive memory; however, unlike the present study, the hippocampus did not show the age-related decline in *GLP-1* (Ohshima et al., 2015). Age-related decline in *GLP-1* might have some bearing on the development of Alzheimer disease in the elderly population.

Species-specific differences in *GLP-1R*

According to Table 3, the *GLP-1R* has been mapped in the rodent brain (Gu et al., 2013) and recently in the nonhuman primate central nervous system (Heppner et al., 2015). *GLP-1R* distribution in the primate brain is similar to that of the rodent with few exceptions. *GLP-1* receptors were absent in the hippocampus and were much more in the amygdala, in the primate brain, when compared with the rodent (Heppner et al., 2015; Ohshima et al., 2015). In animals, the most abundant expression was seen in the hypothalamus.

The *GLP-1R* mRNA mapping of the human brain in the present study highlights many differences when the data is compared to the animal studies. The most important note is the presence of *GLP-1R* mRNA in the different areas of the cortex. Previous studies on monkeys and rats (Heppner et al., 2015; Le et al., 2018; Merchenthaler et al., 1999) did not find *GLP-1R* mRNA in these cortical areas, except in the mouse prefrontal cortex (Ohshima et al., 2015). On the other hand, we did not find *GLP-1R* in the orbitofrontal cortex, though it has been found in the basal portion of the frontal cortex in the rat brain (Merchenthaler et al., 1999). The expression of *GLP-1R* in the hippocampus and hypothalamic paraventricular nucleus is highly conserved between rodents, monkeys, and humans. *GLP-1R* expression in subcortical areas studied in the present study is similar to what is reported in animal studies (Heppner et al., 2015; Le et al., 2018; Merchenthaler et al., 1999; Ohshima et al., 2015). The presence of *GLP-1R* mRNA in the human cerebellum is similar to that found in rats (Rinaman, 2020); however, it is a major deviation from the non-human primate brain

(Heppner et al., 2015). The most abundant expression of *GLP-1R* was seen in the frontal cortex in humans, but in the hypothalamus in animals, this probably denotes higher cerebral control present in humans.

5. Conclusion

To the best of our knowledge, mapping the human brain for *GLP-1* and its receptor has been done for the first time. The quantitative analysis of protein expression has provided data by which the relative significance of different brain regions can be assessed in the context of the *GLP-1*. This information can be utilized for therapeutic application by insight into cellular localization of the *GLP-1* provided by the IHC. This study has provided detailed and novel information about the age-related changes in the *GLP-1* profile. This will aid in understanding the role of *GLP-1* in diseases, such as Alzheimer and Parkinsonism, which are associated with senescence. To understand the species-specific differences in human brain mapping, the data has been compared to the data of primate and non-primate animals. This study is an important step in evaluating the function of *GLP-1* in the brain.

Ethical Considerations

Compliance with ethical guidelines

This study was approved by the Ethics Committee of Post Graduate Institute of Medical Education and Research, on 11.09.2015 (Code: INT/IEC/2015/441).

Funding

This work was supported by the intramural grant under institute research scheme, by Postgraduate Institute of Medical Education and Research [Code: 71/8-Edu-15/694, dated 27/04/2016].

Authors' contributions

Conceptualization, supervision, investigation, writing original draft: Tulika Gupta and Dais Sahni; Methodology: Mandeep Kaur and Devendra Shekhawat; Data collection: Mandeep Kaur and Devendra Shek ha Nanda; Data analysis: Tulika Gupta and Ritu Aggarwal; Writing and editing: Tulika Gupta.

Conflict of interest

The authors declared no conflicts of interest.

Acknowledgments

The authors would like to acknowledge the significant contribution of Arpandeep Randhawa, Harsimran Singh, Ruchi Goyal, Shivani Garg, and Shailon Jyoti, and thank them all.

References

Andersen, A., Lund, A., Knop, F. K., & Vilsbøll, T. (2018). Glucagon-like peptide 1 in health and disease. *Nature Reviews. Endocrinology, 14*(7), 390–403. [DOI:10.1038/s41574-018-0016-2] [PMID]

Gupta, V. (2013). Glucagon-like peptide-1 analogs : An overview. *Indian Journal of Endocrinology and Metabolism, 17*(3), 413–421. [DOI:10.4103/2230-8210.111625] [PMID] [PMCID]

Athauda, D., & Foltynie, T. (2016). The glucagon-like peptide 1 (GLP) receptor as a therapeutic target in Parkinson's disease: Mechanisms of action. *Drug Discovery Today, 21*(5), 802-818. [DOI:10.1016/j.drudis.2016.01.013] [PMID]

Batista, A. F., Bodart-Santos, V., De Felice, F. G., & Ferreira, S. T. (2019). Neuroprotective Actions of Glucagon - Like Peptide - 1 (GLP - 1) Analogues in alzheimer's and Parkinson' s Diseases. *CNS Drugs, 33*(3), 209-223. [DOI:10.1007/s40263-018-0593-6] [PMID]

Farkas, E., Szilvásy-Szabó, A., Ruska, Y., Sinkó, R., Rasch, M. G., & Egebjerg, T., et al. Distribution and ultrastructural localization of the glucagon-like peptide-1 receptor (GLP-1R) in the rat brain. *Brain Structure & Function, 226*(1), 225–245. [PMID]

Gao, C., Liu, Y., Jiang, Y., Ding, J., & Li, L. (2014). Geniposide ameliorates learning memory deficits, reduces tau phosphorylation and decreases apoptosis via GSK3β Pathway in streptozotocin-induced alzheimer rat model. Brain Pathology, 24(3), 261-269. [DOI:10.1111/bpa.12116] [PMID] [PMCID]

Gejl, M., Gjedde, A., Egefjord, L., Møller, A., Hansen, S. B., & Vang, K., et al. (2016). In Alzheimer's disease, 6-month treatment with GLP-1 analog prevents decline of brain glucose metabolism: Randomized, placebo-controlled, double-blind clinical trial. *Frontiers in Aging Neuroscience, 8*, 108. [DOI:10.3389/fnagi.2016.00108] [PMID] [PMCID]

Graham, D. L., Durai, H. H., Trammell, T. S., Noble, B. L., Mortlock, D. P., & Galli, A., et al. (2020). A novel mouse model of glucagon-like peptide-1 receptor expression : A look at the brain. *The Journal of Comparative Neurology, 528*(14), 2445–2470. [DOI:10.1002/cne.24905] [PMID] [PMCID]

Gu, G., Roland, B., Tomaselli, K., Dolman, C. S., Lowe, C., & Heilig, J. S. (2013). Glucagon-like peptide-1 in the rat brain : Distribution of expression and functional implication. *The Journal of Comparative Neurology, 521*(10), 2235–2261 [DOI:10.1002/cne.23282] [PMID]

Heppner, K. M., Kirigiti, M., Secher, A., Paulsen, S. J., Buckingham, R., & Pyke, C., et al. (2015). Expression and distribution of glucagon-like peptide-1 receptor mRNA, protein and binding in the male nonhuman primate (Macaca mulatta) brain. *Endocrinology, 156*(1), 255-267. [DOI:10.1210/en.2014-1675] [PMID]

Holubová, M., Hrubá, L., Popelová, A., Bencze, M., Pražienková, V., & Gengler, S., et al. (2019). Liraglutide and a lipidized analog of prolactin-releasing peptide show neuroprotective effects in a mouse model of β-amyloid pathology. *Neuropharmacology, 144,* 377–387. [DOI:10.1016/j.neuropharm.2018.11.002] [PMID]

Jensen, C. B., Pyke, C., Rasch, M. G., Dahl, A. B., Knudsen, L. B., & Secher, A. (2018). Characterization of the glucagonlike peptide-1 receptor in male mouse brain using a novel antibody and in situ hybridization. *Endocrinology, 159*(2), 665–675. [PMID]

Preston, A. R., & Eichenbaum, H. (2013). Interplay of hippocampus and prefrontal cortex in memory. *Current Biology : CB, 23*(17), R764–R773. [DOI:10.1016/j.cub.2013.05.041.Interplay] [PMID] [PMCID]

Merchenthaler, I., Lane, M., & Shughrue, P. (1999). Distribution of Pre-Pro-glucagon and glucagon-like peptide-1 receptor messenger RNAs in the rat central nervous system. *Journal of Comparative Neurology, 403*(2), 261-280. [DOI:10.1002/(SICI)1096-9861(19990111)403:2<261::AID-CNE8>3.0.CO;2-5]

M de la Monte, S. (2012). Brain Insulin resistance and deficiency as therapeutic targets in alzheimer ' s disease. *Current Alzheimer Research, 9*(1), 35-66. [Link]

Nakajima, S., Numakawa, T., Adachi, N., Yoon, H. S., Odaka, H., & Ooshima, Y., et al. (2016). The inactivation of extracellular signal-regulated kinase by glucagon-like peptide-1 contributes to neuroprotection against oxidative stress. *Neuroscience Letters, 616,* 105-110. [DOI:10.1016/j.neulet.2016.01.052]

Ohshima, R., Hotsumi, K., Holscher, C., & Seki, K. (2015). Age-related decrease in glucagon-like peptide-1 in mouse prefrontal cortex but not in hippocampus despite the preservation of its receptor. *American Journal of BioScience, 3*(1), 11-27. [DOI:10.11648/j.ajbio.20150301.13]

Drucker, D. J. (2018). Mechanisms of action and therapeutic application of glucagon-like peptide-1. *Cell Metabolism, 27*(4), 740-756. [DOI:10.1016/j.cmet.2018.03.001]

Reiner, D. J., Mietlicki-baase, E. G., Mcgrath, L. E., Zimmer, D. J., Bence, K. K., & Sousa, G. L., et al. (2016). Astrocytes regulate GLP-1 receptor-mediated effects on energy balance. *Journal of Neuroscience, 36*(12), 3531-3540. [DOI:10.1523/JNEUROSCI.3579-15.2016] [PMID] [PMCID]

Rinaman, L. (2020). Interoceptive stress activates glucagon-like peptide-1 neurons that project to the hypothalamus. 582-590. *American Journal of Physiology-Regulatory, Integrative and Comparative Physiology, 277*(2), R582-R590. [DOI:10.1152/ajpregu.1999.277.2.R582]

Salcedo, I., Tweedie, D., Li, Y., & Greig, N. H. (2012). Neuroprotective and neurotrophic actions of glucagon-like peptide-1: An emerging opportunity to treat neurodegenerative and cerebrovascular disorders. B*ritish Journal of Pharmacology, 166*(5), 1586-1599. [DOI:10.1111/j.1476-5381.2012.01971.x] [PMID] [PMCID]

Schmittgen, T. D., & Livak, K. J. (2008). Analyzing real-time PCR data by the comparative C_T method. *Nature Protocols, 3*(6), 1101-1108. [DOI:10.1038/nprot.2008.73] [PMID]

Simsir, I. Y., Soyaltin, U. E., & Cetinkalp, S. (2018). Glucagon like peptide-1 (GLP-1) likes Alzheimer's disease. *Diabetes & Metabolic Syndrome: Clinical Research & Reviews, 12*(3), 469-475. [DOI:10.1016/j.dsx.2018.03.002] [PMID]

Trapp, S., & Richards, J. E. (n.d.). The gut hormone glucagon-like peptide-1 produced in brain : Is this physiologically relevant ? *Current Opinion in Pharmacology, 13*(6), 964-969. [DOI:10.1016/j.coph.2013.09.006] [PMID] [PMCID]

This Page Intentionally Left Blank